Structure-preserving reduced order modelling of thermal shallow water equation

Murat Uzunca \cdot Süleyman Yıldız \cdot Bülent Karasözen

Received: date / Accepted: date

Abstract Energy preserving reduced-order models are developed for the rotating thermal shallow water (RTSW) equation in the non-canonical Hamiltonian/Poisson form. The RTSW equation is discretized in space by the skew-symmetric finite-difference operators to preserve the Hamiltonian structure. The resulting system of ordinary differential equations is integrated in time by the energy preserving average vector field (AVF) method. An energy preserving, computationally efficient reduced-order model (ROM) is constructed by proper orthogonal decomposition (POD) with the Galerkin projection. The nonlinearities in the ROM are efficiently computed by discrete empirical interpolation method (DEIM). Preservation of the energy (Hamiltonian), and other conserved quantities; total mass, total buoyancy and total potential vorticity, by the reduced-order solutions are demonstrated which ensures the long term stability of the reduced-order solutions. The accuracy and computational efficiency of the ROMs are shown by a numerical test problem.

Keywords Hamiltonian systems \cdot conserved quantities \cdot finite differences \cdot proper orthogonal decomposition \cdot discrete empirical interpolation

Mathematics Subject Classification (2010) $65M06 \cdot 65P10 \cdot 37J05 \cdot 37M15 \cdot 76B15$

Murat Uzunca

Department of Mathematics, Sinop University, Sinop-Turkey

E-mail: muzunca@sinop.edu.tr

Süleyman Yıldız

Department of Mathematics, Middle East Technical University, Ankara-Turkey

E-mail: yildiz.suleyman@metu.edu.tr

Bülent Karasözen

Institute of Applied Mathematics & Department of Mathematics, Middle East Technical Uni-

versity, Ankara-Turkey

E-mail: bulent@metu.edu.tr

1 Introduction

Rotating shallow water (RSW) equation [30] is a widely used conceptual model in geophysical and planetary fluid dynamics for the behavior of rotating inviscid fluids with one or more layers. Within each layer the horizontal velocity is assumed to be depth-independent, so the fluid moves in columns. However, the RSW model does not allow for gradients of the mean temperature and/or density, which are ubiquitous in the atmosphere and oceans. The rotating thermal shallow water (RTSW) equation [13,32,15,29] represents an extension of the RSW equation, to include horizontal density/temperature gradients both in the atmospheric and oceanic context. The RTSW equation is used, in the general circulation models [37], planetary flows [33], modelling atmospheric and oceanic temperature fronts [14,35], and thermal instabilities [18].

Shallow water equations are discretized on fine space-time grids to obtain high fidelity solutions. Real-time simulations require a large amount of computer memory and computing time. Therefore the computational expense associated with fully resolved simulations remains a barrier in many applications. Model order reduction (MOR) constructs computationally efficient reduced models of largescale dynamical systems by approximating the high-dimensional states, e.g., finite difference, finite-volume, finite-element, spectral elements, discontinuous Galerkin method in low-dimensional subspaces. MOR techniques allow to construct lowdimensional models or reduced-order models (ROMs) for a large-scale dynamical system. The ROMs are computationally efficient and accurate and are worthy when a full-order model (FOM) needs to be simulated multiple-times for different parameter settings. Additionally, ROMs are even more valuable for shallow water equations, in simulating and predicting the model for a very long time horizon. The solutions of the high fidelity FOM, generated by space-time discretization of PDEs, are projected usually on low dimensional reduced spaces using the proper orthogonal decomposition (POD), which is the widely used reduced order modeling technique. Applying POD Galerkin projection, the dominant POD modes of the PDEs are extracted from the snapshots of the FOM solutions. The computation of the FOM and reduced basis are performed in the offline stage, whereas the reduced system is solved in the online stage on the low-dimensional reduced subspace. Projection based intrusive MOR techniques have been intensively applied to the RSW equation in the literature, see, e.g., [5,6,16,20,24,23,2,31].

For nonlinear problems like RTSW equation, the offline/online approach does not generally lead to computational savings. Direct evaluation of nonlinear coefficients requires return to the high-fidelity grid and then projection back to the reduced space. The computational cost is reduced by sampling the nonlinear terms and interpolating them, known as hyper-reduction techniques, such as the discrete empirical interpolation method (DEIM) [3,9]. The efficiency of the ROMs are demonstrated by achieved speed-ups with the POD and DEIM over the FOM solutions. The naive application of POD or DEIM may not preserve the geometric structures, like the symplecticness, energy preservation and passivity of Hamiltonian, Lagrangian and port-Hamiltonian PDEs. The stability of reduced models over long-time integration and the structure-preserving properties has been recently investigated in the context of Lagrangian systems [7], and for port-Hamiltonian systems [8]. For linear and nonlinear Hamiltonian systems, the symplectic model reduction technique, proper symplectic decomposition, is

constructed for Hamiltonian systems like linear wave equation, Sine-Gordon equation, nonlinear Schrödinger equation, to ensure long term stability of the reduced model [1,26]. Recently the average vector field (AVF) method [11] is used as a time integrator to construct reduced order models for Hamiltonian systems like Korteweg-de Vries equation [17,25] and nonlinear Schrödinger equation [19].

In this work, we study reduced order modeling of RTSW equation with preserving the Hamiltonian structure. Replacing the first order derivatives by central finite differences, a skew-gradient system is obtained. The Hamiltonian (energy) and the other conserved quantities, i.e., the Casimirs, are preserved by discretization of the skew-gradient system in time by the AVF method. The skew-symmetric structure of the full order skew-gradient system is preserved using the reduced order technique for Hamiltonian systems with constant Poisson structure [17,19,25]. The full order and reduced order RTSW equations have state-dependent skew-symmetric Poisson matrices, which does not allow separation of online and offline computation of the nonlinear terms. Following [25], we have shown that the complexity of the ROM can be reduced for the POD and for the DEIM. Numerical simulations for the double vortex test case from [15] confirm the structure preserving features of the ROMs, i.e., preservation of the Hamiltonian (energy), total mass, total buoyancy, and total potential vorticity in long term integration.

The paper organized as follows. In Section 2, the RTSW equation is described in Hamiltonian form. The structure preserving FOM obtained by the discretization of RTSW equation in space and time is developed in Section 3. The ROMs with POD and DEIM are constructed in Section 4. In Section 5, results on a numerical example are presented. The paper ends with some conclusions.

2 Thermal shallow water equation

The RTSW equation represents an extension of the RSW equation, to include horizontal density/temperature gradients, known also as Ripa equation [29]. The RTSW equation is obtained along the same lines as the RSW equation, by vertical averaging of the primitive equations in the Boussinesq approximation, and using the hypothesis of columnar motion (mean-field approximation), but relaxing the hypothesis of uniform density/temperature [18,36]. When the layer depth is supposed to be small compared with a typical horizontal length scale, the vertical fluid acceleration in the layer may be neglected. RTSW equation is given for the primitive variables [13,15] as

$$\frac{\partial h}{\partial t} = -(hu)_x - (hv)_y,
\frac{\partial u}{\partial t} = hqv - \left(\frac{u^2 + v^2}{2}\right)_x - \frac{h}{2}s_x - s(h+b)_x
\frac{\partial v}{\partial t} = -hqu - \left(\frac{u^2 + v^2}{2}\right)_y - \frac{h}{2}s_y - s(h+b)_y
\frac{\partial s}{\partial t} = -us_x - vs_y,$$
(1)

where u(x,y,t) and v(x,y,t) are the relative velocities, h(x,y,t) is the fluid height, b(x,y) topographic height, $\rho(x,y,t)$ fluid density, g gravity constant, $s=g\frac{\rho}{\bar{\rho}}$ the

buoyancy, S = hs mass-weighted buoyancy, $q = (v_x - u_y + f)/h$ the potential vorticity with the constant Coriolis force f. The RTSW equation reduces to the RSW equation for constant buoyancy. The RTSW equation (1) is considered on a time interval [0,T] for a final time T > 0, and on a two-dimensional space domain $\Omega \in \mathbb{R}^2$ with periodic boundary conditions. The initial conditions are

$$u(\mathbf{x},0) = u_0(\mathbf{x}), \ v(\mathbf{x},0) = v_0(\mathbf{x}), \ h(\mathbf{x},0) = h_0(\mathbf{x}), \ s(\mathbf{x},0) = s_0(\mathbf{x}),$$

where $\mathbf{x} = (x, y)^T$, and $u_0(\mathbf{x})$, $v_0(\mathbf{x})$, $h_0(\mathbf{x})$ and $s_0(\mathbf{x})$ are given functions. The RTSW equation has similar non-canonical Hamiltonian/Poisson structure as the RSW equation [13,32,15]

$$\frac{\partial z}{\partial t} = -\mathcal{J}(z)\frac{\delta \mathcal{H}}{\delta z} = -\begin{pmatrix} 0 & \partial_x & \partial_y & 0\\ \partial_x & 0 & -q & -h^{-1}s_x\\ \partial_y & q & 0 & -h^{-1}s_y\\ 0 & h^{-1}s_x & h^{-1}s_y & 0 \end{pmatrix}\begin{pmatrix} \frac{u^2 + v^2}{2} + sh + sb\\ hu\\ hv\\ \frac{h^2}{2} + hb \end{pmatrix}, \quad (2)$$

where the Hamiltonian is given by

$$\mathcal{H}(z) = \int_{\Omega} \left(\frac{h^2 s}{2} + h s b + h \frac{u^2 + v^2}{2} \right) d\Omega, \tag{3}$$

with the variational derivatives

$$\frac{\partial \mathcal{H}}{\partial \boldsymbol{u}} = h\boldsymbol{u}, \ \frac{\partial \mathcal{H}}{\partial s} = \frac{1}{2}h^2 + hb, \ \frac{\partial \mathcal{H}}{\partial h} = \frac{1}{2}\boldsymbol{u} \cdot \boldsymbol{u} + sh + sb,$$

The system (2) leads to the RTSW equation (1) with $z = (h, u, v, s)^T$.

The non-canonical Hamiltonian form (2) of the RTSW equation is determined by the skew-symmetric Poisson bracket of two functionals \mathcal{A} and \mathcal{B} [30] as

$$\{\mathcal{A}, \mathcal{B}\} = \iint \left(q \frac{\delta((\mathcal{A}, \mathcal{B}))}{\delta(u, v)} - \frac{\delta \mathcal{A}}{\delta v} \cdot \nabla \frac{\delta \mathcal{B}}{\delta h} + \frac{\delta \mathcal{B}}{\delta v} \cdot \nabla \frac{\delta \mathcal{A}}{\delta h} \right) d\mathbf{x}, \tag{4}$$

where $\nabla = (\partial x, \partial y)^T$, and $\delta \mathcal{A}/\delta v$ is the functional derivative of \mathcal{A} with respect to v. The functional Jacobian is given by

$$\frac{\delta((\mathcal{A},\mathcal{B})}{\delta(u,v)} = \frac{\delta\mathcal{A}}{\delta u} \frac{\delta\mathcal{B}}{\delta v} - \frac{\delta\mathcal{B}}{\delta u} \frac{\delta\mathcal{A}}{\delta v}.$$

The Poisson bracket (4) is related to the skew-symmetric Poisson matrix \mathcal{J} as $\{\mathcal{A},\mathcal{B}\}=\{\mathcal{A},\mathcal{J}\mathcal{B}\}$. Although the matrix \mathcal{J} in (2) is not skew-symmetric, the skew-symmetry of the Poisson bracket appears after integrations by parts, and the Poisson bracket satisfies the Jacobi identity

$$\{\mathcal{A}, \{\mathcal{B}, \mathcal{D}\}\} + \{\mathcal{B}, \{\mathcal{D}, \mathcal{A}\}\} + \{\mathcal{A}, \{\mathcal{B}, \mathcal{D}\}\} = 0,$$

for any three functionals \mathcal{A} , \mathcal{B} and \mathcal{D} . Conservation of the Hamiltonian (3) follows from the antisymmetry of the Poisson bracket (4)

$$\frac{d\mathcal{H}}{dt} = \{\mathcal{H}, \mathcal{H}\} = 0.$$

Other conserved quantities are the Casimirs which are additional constants of motion, and commute with any functional A, i.e., the Poisson bracket vanishes

$$\{\mathcal{A}, \mathcal{C}\} = 0, \quad \forall \mathcal{A}(\mathbf{z}) \quad \text{or} \quad \mathcal{J}^{ij} \frac{\partial \mathcal{C}}{\partial \mathbf{z}^j} = 0.$$

The Casimirs of the RTSW equation are the total mass, the total potential vorticity, and the total buoyancy

$$\mathcal{M} = \int h \ d\Omega, \quad \mathcal{Q} = \int hq \ d\Omega, \quad \mathcal{B} = \int hs \ d\Omega.$$
 (5)

Unlike the RSW equation, the potential enstropy is not conserved.

3 Full order discretization

The RTSW equation (2) is discretized by finite differences on a uniform grid in the rectangular spatial domain $\Omega=(a,b)\times(c,d)$ with the nodes $\boldsymbol{x}_{ij}=(x_i,y_j)^T$, where $x_i=a+(i-1)\Delta x$ and $y_j=c+(j-1)\Delta y,\,i=1,\ldots,n_x+1,\,j=1,\ldots,n_y+1$. The semi-discrete state variables are given as

$$h(t) = (h_{11}(t), \dots, h_{1n_y}(t), h_{21}(t), \dots, h_{2n_y}(t), \dots, h_{n_x n_y}(t))^T,$$

$$u(t) = (u_{11}(t), \dots, u_{1n_y}(t), u_{21}(t), \dots, u_{2n_y}(t), \dots, u_{n_x n_y}(t))^T,$$

$$v(t) = (v_{11}(t), \dots, v_{1n_y}(t), v_{21}(t), \dots, v_{2n_y}(t), \dots, v_{n_x n_y}(t))^T,$$

$$s(t) = (s_{11}(t), \dots, s_{1n_y}(t), s_{21}(t), \dots, s_{2n_y}(t), \dots, s_{n_x n_y}(t))^T.$$
(6)

The solution vector is defined by $\mathbf{z}(t) = (\mathbf{h}(t), \mathbf{u}(t), \mathbf{v}(t), \mathbf{s}(t)) : [0, T] \mapsto \mathbb{R}^{4n}$. We note that the degree of freedom is given by $n = n_x n_y$ because of the periodic boundary conditions, i.e., the most right and the most top grid nodes are not included. Throughout the paper, we do not explicitly represent the time dependency of the semi-discrete solutions for simplicity, and we write $\mathbf{u}, \mathbf{v}, \mathbf{h}, \mathbf{s}$, and \mathbf{z} .

The first order derivatives in space are approximated by one dimensional central finite differences in x and y directions, respectively, and they are extended to two dimensions utilizing the Kronecker product. Let \widetilde{D}_p be the matrix containing the central finite differences under periodic boundary conditions

$$\widetilde{D}_{p} = \begin{pmatrix} 0 & 1 & & -1 \\ -1 & 0 & 1 & & \\ & \ddots & \ddots & \ddots & \\ & & -1 & 0 & 1 \\ 1 & & & 1 & 0 \end{pmatrix} \in \mathbb{R}^{p \times p}.$$

Then, on the two dimensional mesh, the central finite difference matrices corresponding to the first order partial derivatives ∂_x and ∂_y are given respectively by

$$D_x = \frac{1}{2\Delta x} \widetilde{D}_{n_x} \otimes I_{n_y} \in \mathbb{R}^{n \times n} , \quad D_y = \frac{1}{2\Delta y} I_{n_x} \otimes \widetilde{D}_{n_y} \in \mathbb{R}^{n \times n},$$

where \otimes denotes the Kronecker product, and I_{n_x} and I_{n_y} are the identity matrices of size n_x and n_y , respectively.

The semi-discretization of the RTSW equation (2) leads to a 4n-dimensional system of Hamiltonian ODEs in skew-gradient form

$$\frac{dz}{dt} = -J(z)\nabla_z H(z),\tag{7}$$

with the skew-symmetric Poisson matrix and the discrete gradient Hamiltonian given by

$$J(\boldsymbol{z}) = \begin{pmatrix} 0 & D_x & D_y & 0 \\ D_x & 0 & -\boldsymbol{q}^d & -(\boldsymbol{h}^{-1} \circ (D_x \boldsymbol{s}))^d \\ D_y & \boldsymbol{q}^d & 0 & -(\boldsymbol{h}^{-1} \circ (D_y \boldsymbol{s}))^d \\ 0 & (\boldsymbol{h}^{-1} \circ (D_x \boldsymbol{s}))^d & (\boldsymbol{h}^{-1} \circ (D_y \boldsymbol{s}))^d & 0 \end{pmatrix},$$

$$\nabla_{\boldsymbol{z}} H(\boldsymbol{z}) = \begin{pmatrix} \frac{\boldsymbol{u}^2 + \boldsymbol{v}^2}{2} + \boldsymbol{s} \circ \boldsymbol{h} + b\boldsymbol{s} \\ \boldsymbol{h} \circ \boldsymbol{u} \\ \boldsymbol{h} \circ \boldsymbol{v} \\ \frac{1}{2}\boldsymbol{h}^2 + b\boldsymbol{h} \end{pmatrix},$$

where \circ denotes element-wise or Hadamard product, and the square operations are also held element-wise. The matrix $\mathbf{q}^d \in \mathbb{R}^{n \times n}$ is the diagonal matrix with the diagonal elements $\mathbf{q}_{ii}^d = \mathbf{q}_i$ where \mathbf{q} is the semi-discrete vector of the potential vorticity $q, i = 1, \ldots, n$. The diagonal matrices of the vectors $\mathbf{h}^{-1} \circ (D_x \mathbf{s})$ and $\mathbf{h}^{-1} \circ (D_y \mathbf{s})$ are defied similarly.

For the time integration we use the Poisson structure preserving AVF method [11]. The AVF method is used with finite element discretization of the RSW equation [4,34] and for the linearized RTSW equation [15] in Poisson form. The time interval [0,T] is partitioned into K uniform meshes with the step size $\Delta t = T/K$ as $0=t_0 < t_1 < \ldots < t_K = T$, and $t_k = k\Delta t$, $k=0,1,\ldots,K$. The fully discrete solution vector at time t_k is denoted as $\boldsymbol{h}^k = \boldsymbol{h}(t_k)$. Similar setting is used for the other state variables. Integration of the semi-discrete RTSW equation (7) in time by the AVF integrator leads to the fully discrete problem

$$\boldsymbol{z}^{k+1} = \boldsymbol{z}^k + \Delta t J \left(\frac{\boldsymbol{z}^{k+1} + \boldsymbol{z}^k}{2} \right) \int_0^1 \nabla_{\boldsymbol{z}} H(\xi(\boldsymbol{z}^{k+1} - \boldsymbol{z}^k) + \boldsymbol{z}^k) d\xi \tag{8}$$

for $k = 0, 1, \dots, K - 1$.

Practical implementation of the AVF method requires the evaluation of the integral on the right-hand side of (8). Since the Hamiltonian \mathcal{H} and Casimirs are polynomials of degree at most 3, they can be exactly integrated with the symmetric Gaussian quadrature rule of order 2.

The full discrete forms of the energy, total mass, total potential vorticity, and total buoyancy are given at the time instance t_k as

$$H^{k}(\boldsymbol{z}) = \sum_{i=1}^{n} \left(\frac{1}{2} (\boldsymbol{h}_{i}^{k})^{2} \boldsymbol{s}_{i}^{k} + \boldsymbol{h}_{i}^{k} \boldsymbol{s}_{i}^{k} b + \boldsymbol{h}_{i}^{k} \frac{(\boldsymbol{u}_{i}^{k})^{2} + (\boldsymbol{v}_{i}^{k})^{2}}{2} \right) \Delta x \Delta y,$$

$$M^{k}(\boldsymbol{z}) = \sum_{i=1}^{n} \boldsymbol{h}_{i}^{k} \Delta x \Delta y,$$

$$Q^{k}(\boldsymbol{z}) = \sum_{i=1}^{n} \left((D_{x} \boldsymbol{v}^{k})_{i} - (D_{y} \boldsymbol{u}^{k})_{i} + f \right) \Delta x \Delta y,$$

$$B^{k}(\boldsymbol{z}) = \sum_{i=1}^{n} \boldsymbol{h}_{i}^{k} \boldsymbol{s}_{i}^{k} \Delta x \Delta y.$$

$$(9)$$

The AVF method preserves Hamiltonian (energy) and the quadratic Casimir functions, i.e., the total potential vorticity, and the total buoyancy [11]. Linear conserved quantities like the total mass are preserved by all time-integrators including the AVF method.

We remark that recently the RTSW equation as a hyperbolic system was solved with the well-balanced finite volume method in [22,21].

4 Reduced-order model

The RTSW equation is a non-canonical Hamiltonian PDE with a state-dependent Poisson structure, and a straightforward application of the POD will not preserve the skew-gradient structure of the RTSW equation (7) in reduced form. In this section, we construct ROMs that preserve the skew-gradient structure of the semi-discrete RTSW equation (7), and consequently the discrete conserved quantities in (9). Energy preserving POD reduced systems are constructed for Hamiltonian systems with constant skew-symmetric matrices like the Korteweg-de Vries equation [17,25] and nonlinear Schrödinger equation (NLSE) [19]. The approach in [17] can be applied to skew-gradient systems with state-dependent skew-symmetric structure as the NTSW equation (7). We show that the state-dependent skew-symmetric matrix in (7) can be evaluated efficiently in the online stage independent of the full dimension n. The full and reduced models are computed separately approximating the nonlinear terms by DEIM. The DEIM also preserves the skew-symmetric form as shown for the NLSE [19].

The POD basis vectors are obtained usually by stacking all state variables in one vector and a commonly reduced subspace is computed by taking the singular value decomposition (SVD) of snapshot data. Because the governing PDEs like the RTSW equation are coupled, the resulting ROMs do not preserve the coupling structure of the FOM and produce unstable reduced-order solutions [27,28]. In order to maintain the coupling structure in the ROMs, the POD basis vectors are computed separately for each of the state vectors $\boldsymbol{h}, \boldsymbol{u}, \boldsymbol{v}$ and \boldsymbol{s} .

The POD basis is computed through the mean subtracted snapshot matrices S_u , S_v , S_h and S_s , constructed by the solutions of the full discrete high fidelity

model (8)

$$egin{aligned} \mathsf{S}_u &= \left(oldsymbol{u}^1 - \overline{oldsymbol{u}}, \cdots, oldsymbol{u}^K - \overline{oldsymbol{u}}
ight) \in \mathbb{R}^{n imes K}, \ \mathsf{S}_v &= \left(oldsymbol{v}^1 - \overline{oldsymbol{v}}, \cdots, oldsymbol{v}^K - \overline{oldsymbol{v}}
ight) \in \mathbb{R}^{n imes K}, \ \mathsf{S}_h &= \left(oldsymbol{h}^1 - \overline{oldsymbol{h}}, \cdots, oldsymbol{h}^K - \overline{oldsymbol{h}}
ight) \in \mathbb{R}^{n imes K}, \ \mathsf{S}_s &= \left(oldsymbol{s}^1 - \overline{oldsymbol{s}}, \cdots, oldsymbol{s}^K - \overline{oldsymbol{s}}
ight) \in \mathbb{R}^{n imes K}, \end{aligned}$$

where \overline{u} , \overline{v} , \overline{h} , $\overline{s} \in \mathbb{R}^n$ denote the time averaged means of the solutions

$$\overline{\boldsymbol{u}} = \frac{1}{K} \sum_{k=0}^K \boldsymbol{u}^k \;,\; \overline{\boldsymbol{v}} = \frac{1}{K} \sum_{k=0}^K \boldsymbol{v}^k \;,\; \overline{\boldsymbol{h}} = \frac{1}{K} \sum_{k=0}^K \boldsymbol{h}^k ,\; \overline{\boldsymbol{s}} = \frac{1}{K} \sum_{k=0}^K \boldsymbol{s}^k .$$

The mean-subtracted ROM is used frequently in fluid dynamics to stabilize the reduced system, and it guarantees that the ROM solutions would satisfy the same boundary conditions as for the FOM [5].

The POD modes are computed by applying SVD to the snapshot matrices

$$\mathbf{S}_u = W_u \boldsymbol{\varSigma}_u \boldsymbol{U}_u^T \quad \mathbf{S}_v = W_v \boldsymbol{\varSigma}_v \boldsymbol{U}_v^T, \quad \mathbf{S}_h = W_h \boldsymbol{\varSigma}_h \boldsymbol{U}_h^T, \quad \mathbf{S}_s = W_s \boldsymbol{\varSigma}_s \boldsymbol{U}_s^T,$$

where for $i=u,v,h,s,\ W_i\in\mathbb{R}^{n\times K}$ and $U_i\in\mathbb{R}^{K\times K}$ are orthonormal matrices, and $\Sigma_i\in\mathbb{R}^{K\times K}$ is the diagonal matrix with its diagonal entries are the singular values $\sigma_{i,1}\geq\sigma_{i,2}\geq\cdots\geq\sigma_{i,K}\geq0$. The matrices $V_{i,N_i}\in\mathbb{R}^{n\times N_i}$ of rank N_i POD modes consists of the first N_i left singular vectors from W_i corresponding to the N_i largest singular values, which satisfies the following least squares error

$$\min_{V_{i,N_i} \in \mathbb{R}^{n \times N_i}} || \mathbf{S}_i - V_{i,N_i} V_{i,N_i}^T \mathbf{S}_i ||_F^2 = \sum_{j=N_i+1}^K \sigma_{i,j}^2 \;, \quad i = u, v, h, s,$$

where $\|\cdot\|_F$ is the Frobenius norm. In the sequel, we omit the subscript N_i from the POD matrices V_{i,N_i} , and we write V_i for easy notation. Moreover, we have the reduced approximations

$$u \approx \overline{u} + V_u u_r, \quad v \approx \overline{v} + V_v v_r, \quad h \approx \overline{h} + V_h h_r, \quad s \approx \overline{s} + V_s s_r,$$
 (10)

where the vectors u_r , u_r , h_r and s_r are the ROM solutions obtained by Galerkin projection onto the reduced space

$$\frac{d}{dt}z_r = V_z^T J(z) \nabla_z H(z), \tag{11}$$

where $z_r = (h_r, u_r, v_r, s_r)$. The block diagonal matrix V_z in (11) contains the matrix of POD modes for each state variable

$$V_z = \begin{pmatrix} V_h & & \\ & V_u & \\ & & V_v \\ & & & V_s \end{pmatrix} \in \mathbb{R}^{4n \times (N_h + N_u + N_v + N_s)}.$$

The skew-gradient structure of the FOM (7) is not preserved by the ROM (11). A reduced skew-gradient system is obtained formally by inserting $V_z V_z^T$ between J(z) and $\nabla_z H(z)$ [17], leading to the ROM

$$\frac{d}{dt}z_r = J_r(z)\nabla_{\mathbf{z}_r}H(z),\tag{12}$$

where $J_r(z) = V_z^T J(z) V_z$ and $\nabla_{\mathbf{z}_r} H(z) = V_z^T \nabla_{\mathbf{z}} H(z)$. The reduced order RTSW equation (12) is also solved by the AVF method.

The skew-symmetric matrix $J_r(z)$ in the reduced order RTSW equation (12) can be written explicitly as

$$J_{r}(z) = \begin{pmatrix} 0 & -V_{h}^{T} D_{x} V_{u} & -V_{h}^{T} D_{y} V_{v} & 0 \\ -V_{u}^{T} D_{x} V_{h} & 0 & V_{u}^{T} \boldsymbol{q}^{d} V_{v} & V_{u}^{T} (\boldsymbol{h}^{-1} \circ (D_{x} \boldsymbol{s}))^{d} V_{s} \\ -V_{v}^{T} D_{y} V_{h} & -V_{v}^{T} \boldsymbol{q}^{d} V_{u} & 0 & V_{v}^{T} (\boldsymbol{h}^{-1} \circ (D_{x} \boldsymbol{s}))^{d} V_{s} \\ 0 & -V_{s}^{T} (\boldsymbol{h}^{-1} \circ (D_{x} \boldsymbol{s}))^{d} V_{u} - V_{s}^{T} (\boldsymbol{h}^{-1} \circ (D_{y} \boldsymbol{s}))^{d} V_{v} & 0 \end{pmatrix}.$$

The block matrices in $J_r(z)$ are constant, which can be precomputed in the offline stage, but the matrices containing the terms \mathbf{q}^d , $\mathbf{h}^{-1} \circ (D_x s)$ and $\mathbf{h}^{-1} \circ (D_y s)$ are not constant and should be computed in the online stage depending on the full order system. Exploiting the diagonal structure of \mathbf{q}^d (the same procedure is followed for the terms $\mathbf{h}^{-1} \circ (D_x s)$ and $\mathbf{h}^{-1} \circ (D_y s)$), the computational complexity of evaluating the state dependent skew-symmetric matrix $J_r(z)$ in (12) can be reduced similar to the skew-gradient systems with constant skew-symmetric matrices as in [25]. Let $\operatorname{vec}(\cdot)$ denotes the vectorization of a matrix. For any $A \in \mathbb{R}^{m \times n}$ and $B \in \mathbb{R}^{n \times p}$

$$\operatorname{vec}(AB) = (I_p \otimes A)\operatorname{vec}(B) = (B^{\top} \otimes I_m)\operatorname{vec}(A).$$

Thus, for a diagonal matrix $D \in \mathbb{R}^{n \times n}$ and $V \in \mathbb{R}^{n \times r}$

$$\operatorname{vec}(V^{\top}DV) = (I_r \otimes V^{\top})\operatorname{vec}(DV)$$

$$= (I_r \otimes V^{\top})(V^{\top} \otimes I_n)\operatorname{vec}(D)$$

$$= (V \otimes V)^{\top}\operatorname{vec}(D)$$

$$= (V \otimes V)^{\top}M^{\top}\tilde{D}$$

$$= \begin{pmatrix} V(1,:) \otimes V(1,:) \\ \vdots \\ V(n,:) \otimes V(n,:) \end{pmatrix}^{\top}\tilde{D},$$

where $M \in \mathbb{R}^{n \times n^2}$ is a matrix satisfying $M(a \otimes b) = a \circ b$ for any vector $a, b \in \mathbb{R}^n$, and $\tilde{D} = [D_{11}, D_{22}, \dots, D_{nn}]^T \in \mathbb{R}^n$. Using the above result, the computational complexity of the matrix products $V_u^T \mathbf{q}^d V_v$ and $V_v^T \mathbf{q}^d V_u$ is reduced from $\mathcal{O}(nN(n+N))$ to $\mathcal{O}(nN^2)$, where $N = \max\{N_u, N_v\}$.

Due to the nonlinear terms, the computation of the reduced system (12) still scales with the dimension n of the FOM. This can be reduced by applying a hyper-reduction technique such as DEIM [9]. The ROM (12) can be rewritten as a nonlinear ODE system of the following form

$$\frac{d}{dt}\boldsymbol{z}_{r} = V_{z}^{T}F(\boldsymbol{z}) = \begin{pmatrix} V_{h}^{T}F_{1}(\boldsymbol{z}) \\ V_{u}^{T}F_{2}(\boldsymbol{z}) \\ V_{v}^{T}F_{3}(\boldsymbol{z}) \\ V_{s}^{T}F_{4}(\boldsymbol{z}) \end{pmatrix}.$$
(13)

The DEIM procedure, originally introduced in [9], is utilized to approximate the nonlinear vectors $F_j(\mathbf{z}(t))$ in (13) by interpolating them onto an empirical basis, that is,

$$F_j(\boldsymbol{z}) \approx \Phi^{(j)} c^{(j)}(t), \quad j = 1, \dots, 4,$$

where $\{\phi_1^{(j)},\ldots,\phi_{p_j}^{(j)}\}\subset\mathbb{R}^n$ is a low dimensional basis, $\Phi^{(j)}=[\phi_1^{(j)},\ldots,\phi_{p_j}^{(j)}]\in\mathbb{R}^{n\times p_j}$, and $\mathbf{c}^{(j)}(t):[0,T]\mapsto\mathbb{R}^{p_j}$ is the vector of time-dependent coefficients to be determined.

Let $\mathsf{P}^{(j)} = [e_{\rho_1}^{(j)}, \dots, e_{\rho_p}^{(j)}] \in \mathbb{R}^{n \times p_j}$ be a subset of columns of the identity matrix, named as the "selection matrix". If $(\mathsf{P}^{(j)})^{\top} \varPhi^{(j)}$ is invertible, in [9] the coefficient vector $\mathsf{c}^{(j)}(t)$ is uniquely determined by solving the linear system $(\mathsf{P}^{(j)})^{\top} \varPhi^{(j)} \mathsf{c}^{(j)}(t) = (\mathsf{P}^{(j)})^{\top} F_j(\mathbf{z}(t))$, so that the nonlinear terms in the reduced model (13) are approximated by

$$F_{i}(\mathbf{z}(t)) \approx \Phi^{(j)} \mathsf{c}^{(j)}(t) = \Phi^{(j)} ((\mathsf{P}^{(j)})^{\top} \Phi^{(j)})^{-1} (\mathsf{P}^{(j)})^{\top} F_{i}(\mathbf{z}(t)). \tag{14}$$

The accuracy of DEIM depends mainly on the basis choice, and not much by the choice of $\mathsf{P}^{(j)}$. In most applications the interpolation basis $\{\phi_1^{(j)},\ldots,\phi_p^{(j)}\}$ is selected as the POD basis of the set of snapshots matrices of the nonlinear vectors given by

$$G_j = (F_j^1, F_j^2, \dots, F_j^K) \in \mathbb{R}^{n \times K}, \quad j = 1, \dots, 4,$$
 (15)

where $F_j^k = F_j(\boldsymbol{z}^k)$ denotes the j-th vector component of the nonlinearity $F(\boldsymbol{z})$ in (13) at time t_k , computed by the use of the FOM solution vectors $\boldsymbol{z}^k = \boldsymbol{z}(t_k)$, $k = 1, \ldots, K$. The columns of the matrices $\Phi^{(j)} = [\phi_1^{(j)}, \ldots, \phi_{p_j}^{(j)}]$ are determined as the first $p_j \ll n$ dominant left singular vectors in the SVD of G_j . The selection matrix $P^{(j)}$ for DEIM is determined by a greedy algorithm based on the system residual; see [9, Algorithm 3.1]. Another approach called Q-DEIM [38], is shown to lead to better accuracy and stability properties of the computed selection matrix $P^{(j)}$, where the authors use a pivoted QR-factorization of $(\Phi^{(j)})^{\top}$. In the sequel, we use Q-DEIM for the calculation of the selection matrix $P^{(j)}$, see Algorithm 1.

Algorithm 1 Q-DEIM

- 1: **Input:** Basis matrix $\Phi \in \mathbb{R}^{n \times p}$, $p \ll n$
- 2: Output: Selection matrix P
- 3: Perform pivoted QR factorization of Φ^{\top} so that $\Phi^{\top}\Pi = QR$
- 4: Set $P = \Pi(:, 1:p)$

Using the DEIM approximations in (14), the ROM (13) takes the form

$$\frac{d}{dt}z_r = \begin{pmatrix} \mathcal{V}_{h,1}F_{r,1}(z) \\ \mathcal{V}_{u,2}F_{r,2}(z) \\ \mathcal{V}_{v,3}F_{r,3}(z) \\ \mathcal{V}_{s,3}F_{r,4}(z) \end{pmatrix},$$
(16)

where

$$\mathcal{V}_{i,j} = V_i^T \varPhi^{(j)} \big((\mathsf{P}^{(j)})^T \varPhi^{(j)} \big)^{-1}, \quad (i,j) = (h,1), (u,2), (v,3), (s,4),$$

are all matrices of size $N_i \times p_j$, which are precomputed in the offline stage, and the reduced nonlinearities $F_{r,j}(\mathbf{z}) = (\mathsf{P}^{(j)})^T F_j(\mathbf{z})$ are computed by considering just $p_j \ll n$ entries of the nonlinearities $F_j(\mathbf{z})$ among n entries, j=1,2,3,4. In addition, being an approximation to the right hand side of the ROM (13), the ROM (16) with DEIM approximately preserves the skew-gradient structure, but exactly at the interpolation points.

5 Numerical results

We consider the double vortex test case from [15] on the doubly periodic space domain $\Omega = [0, L]^2$ without the bottom topography (b = 0). The initial conditions are given by

$$h = H_0 - \Delta h \left[e^{-0.5((x_1')^2 + (y_1')^2)} + e^{-0.5((x_2')^2 + (y_2')^2)} - \frac{4\pi\sigma_x\sigma_y}{L^2} \right],$$

$$u = \frac{-g\Delta h}{f\sigma_y} \left[y_1'' e^{-0.5((x_1')^2 + (y_1')^2)} + y_2'' e^{-0.5((x_2')^2 + (y_2')^2)} \right],$$

$$v = \frac{g\Delta h}{f\sigma_x} \left[x_1'' e^{-0.5((x_1')^2 + (y_1')^2)} + x_2'' e^{-0.5((x_2')^2 + (y_2')^2)} \right],$$

$$s = g \left(1 + 0.05 \sin \left[\frac{2\pi}{L} (x - xc) \right] \right)$$

where xc = 0.5L and

$$x'_{1} = \frac{L}{\pi \sigma_{x}} \sin \left[\frac{\pi}{L}(x - xc_{1})\right], \qquad x'_{2} = \frac{L}{\pi \sigma_{x}} \sin \left[\frac{\pi}{L}(x - xc_{2})\right],$$

$$y'_{1} = \frac{L}{\pi \sigma_{y}} \sin \left[\frac{\pi}{L}(y - yc_{1})\right], \qquad y'_{2} = \frac{L}{\pi \sigma_{y}} \sin \left[\frac{\pi}{L}(y - yc_{2})\right]$$

$$x''_{1} = \frac{L}{2\pi \sigma_{x}} \sin \left[\frac{2\pi}{L}(x - xc_{1})\right], \qquad x''_{2} = \frac{L}{2\pi \sigma_{x}} \sin \left[\frac{2\pi}{L}(x - xc_{2})\right],$$

$$y''_{1} = \frac{L}{2\pi \sigma_{y}} \sin \left[\frac{2\pi}{L}(y - yc_{1})\right], \qquad y''_{2} = \frac{L}{2\pi \sigma_{y}} \sin \left[\frac{2\pi}{L}(y - yc_{2})\right]$$

The center of vorticities are given by

$$xc_1 = (0.5 - ox)L$$
, $xc_2 = (0.5 + ox)L$, $yc_1 = (0.5 - oy)L$, $yc_2 = (0.5 + oy)L$.

The parameters are taken as $L=5000 \mathrm{km}$, $f=0.00006147 \mathrm{s}^{-1}$, $H_0=75 \mathrm{m}$, $h=75 \mathrm{m}$, $g=9.80616 \mathrm{ms}^{-2}$, $\sigma_x=\sigma_y=\frac{3}{40} L$ and ox=oy=0.1. The simulations are performed for 250 iterations with the step-size $\Delta t=486$. The spatial mesh sizes are taken as $\Delta x=\Delta y=50 \mathrm{km}$. The resulting snapshot matrices for each state variable have the size 10000×250 .

The POD and DEIM basis are truncated according to the following relative cumulative energy criterion

$$\min_{p} \frac{\sum_{j=1}^{p} \sigma_{j}^{2}}{\sum_{j=1}^{K} \sigma_{j}^{2}} > 1 - \kappa, \tag{17}$$

where κ is a user-specified tolerance, and σ_j are the singular values. In our simulations, we set $\kappa = 10^{-3}$ and $\kappa = 10^{-5}$ to catch at least 99.9% and 99.999% of relative cumulative energy for POD and DEIM modes, respectively.

The time averaged relative errors between FOM and ROM solutions are given for each of the state variable w = u, v, h, s in the time-averaged L^2 -norm as

$$\|\boldsymbol{w} - \widehat{\boldsymbol{w}}\|_{rel} = \frac{1}{N_t} \sum_{k=1}^{N_t} \frac{\|\boldsymbol{w}^k - \widehat{\boldsymbol{w}}^k\|_{L^2}}{\|\boldsymbol{w}^k\|_{L^2}}, \quad \|\boldsymbol{w}^k\|_{L^2}^2 = \sum_{i=1}^{N} (\boldsymbol{w}_i^k)^2 \Delta x \Delta y,$$

where $\hat{\boldsymbol{w}} = \overline{\boldsymbol{w}} + V_w \boldsymbol{w}_r$ denotes the reduced approximation to \boldsymbol{w} .

Conservation of the discrete conserved quantities (9): energy, mass, buoyancy, and total vorticity, by the FOM solutions and the ROM solutions are measured using the time-averaged absolute error

$$\|\mathbf{w}\|_{E} = \frac{1}{K} \sum_{k=1}^{K} |E^{k}(\mathbf{w}) - E^{0}(\mathbf{w})|, \quad E = H, M, B, Q.$$

All simulations are performed on a machine with Intel[®] CoreTM i7 2.5 GHz 64 bit CPU, 8 GB RAM, Windows 10, using 64 bit MatLab R2014.

In Figure 1, the singular values decay slowly for both the state variables and nonlinear terms, which is the characteristic of the problems with complex wave phenomena in fluid dynamics. According to the energy criteria (17), we select $N_h = 12$, $N_u = 7$, $N_v = 11$, $N_s = 3$ POD modes and $p_j = 53$ DEIM modes, $j = 1, \ldots, 4$. A large number of DEIM modes are needed for convergence of the Newton method for solving the reduced system (12).

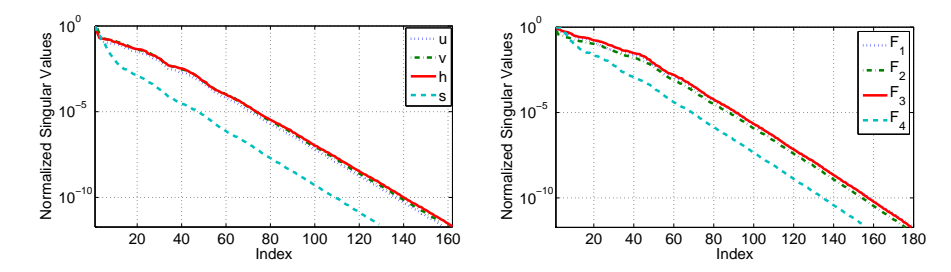


Fig. 1: Normalized singular values: (left) state variables, (right) nonlinear terms

The a priori error bounds for the ROM solutions are proportional to the sums of the singular values corresponding to neglected POD and DEIM modes [10]. As shown in Figures 2 and 3, the bouyancy \boldsymbol{s} and the potential vorticity \boldsymbol{q} are well approximated by the ROMs at the final time.

In Figure 4, the Hamiltonian (energy) error $|H^k - H^0|$, total mass error $|M^k - M^0|$, total buoyancy error $|B^k - B^0|$, and the total potential vorticity error $|Q^k - Q^0|$ are plotted, at the discrete time steps $k = 1, \ldots, K$. The total mass and the total potential vorticity are preserved up to machine precision. The energy and the total buoyancy errors of the FOMs and ROMs show bounded oscillations over time, i.e., they are preserved approximately at the same level of accuracy.

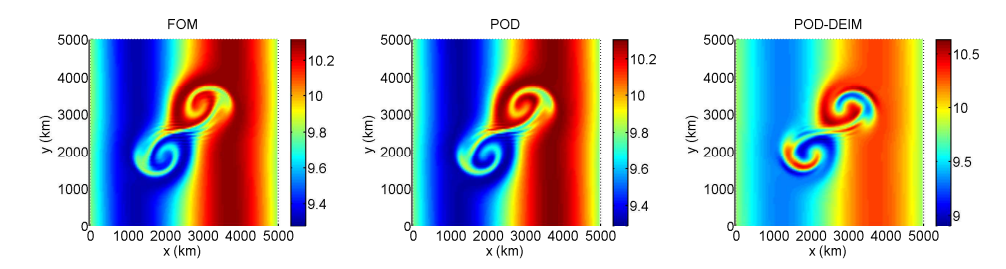


Fig. 2: Bouyancy of the FOMs and ROMs at the final time T=250

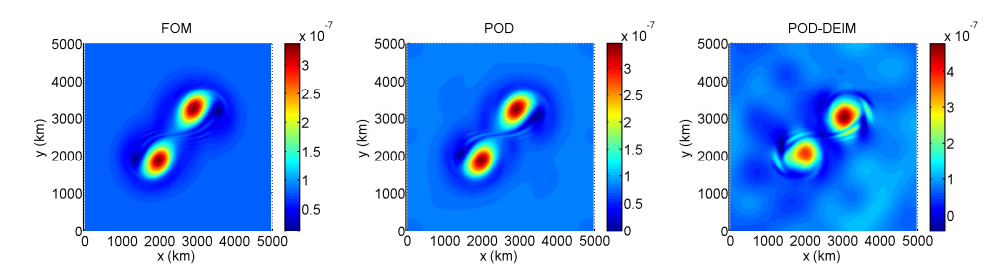


Fig. 3: Potential vorticity of the FOMs and ROMs at the final time T=250

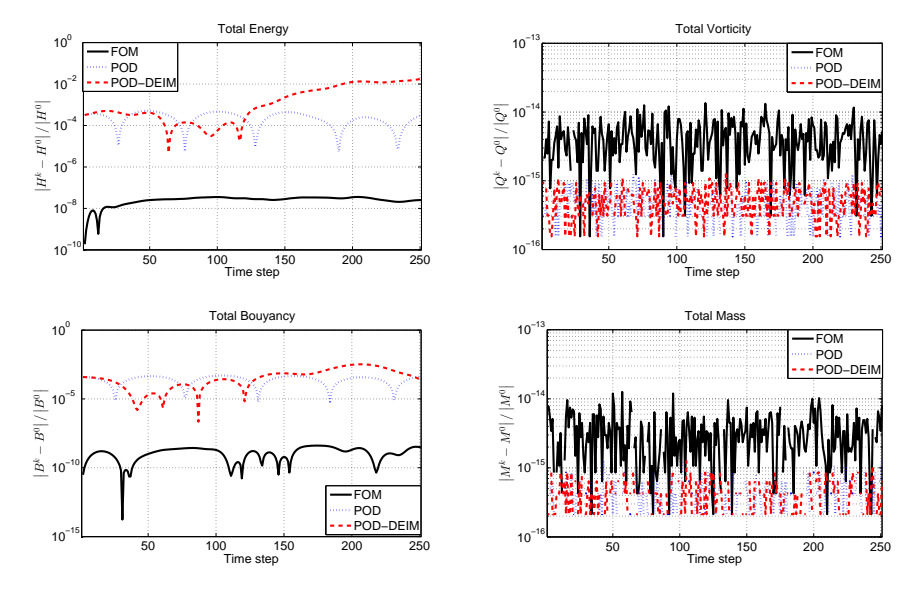


Fig. 4: Errors of conserved quantities for FOMs and ROMs

The time-averaged relative L_2 -errors of the FOM and ROM solutions in Table 1 are at the same level of accuracy for the POD and POD-DEIM. The conserved quantities are also accurately preserved by the ROMs as shown in Table 2. The

POD-DEIM errors are slightly larger than the POD errors in both Tables, but the POD-DEIM is much faster than the POD as shown in Table 3.

Table 1: Time-averaged relative L_2 -errors of the state variables

	$\ oldsymbol{h} - \widehat{oldsymbol{h}}\ _{rel}$	$\ oldsymbol{u}-\widehat{oldsymbol{u}}\ _{rel}$	$\ oldsymbol{v}-\widehat{oldsymbol{v}}\ _{rel}$	$\ oldsymbol{s}-\widehat{oldsymbol{s}}\ _{rel}$
POD	6.201e-03	9.275e-02	1.075e-01	9.857e-04
POD-DEIM	3.904e-02	5.754e-01	9.074e-01	2.507e-03

Table 2: Mean absolute errors between the conserved quantities by FOM and ${
m ROMs}$

	Energy	Total potential vorticity	Total mass	Total buoyancy
POD	2.5498e-04	3.9893e-15	2.9558e-15	2.7948e-04
POD-DEIM	4.2767e-03	3.9509e-15	2.9660e-15	7.3204e-04

In Table 3, basis computation includes SVD computation, and online computation consists of time needed for projection and solution of the reduced system. The speed-up factors in Table 3 show that the ROMs with DEIM increases the computational efficiency much further.

Table 3: CPU time (in seconds) and speed-up factors

		CPU Time	Speed-up
FOM		1198.27	
POD	basis computation	5.14	
	online computation	51.26	23.4
POD-DEIM	basis computation (POD+DEIM)	11.03	
	online computation	11.19	107.1

6 Conclusions

In this paper, the Hamiltonian/energy reduced order modeling is developed for the RTSW equation. The accuracy and computational efficiency of the reduced solutions are shown on a numerical test problem. Preservation of the energy and other conserved quantities demonstrate the stability of the reduced solutions in long time integration. As a future study, we plan to apply this methodology to the magnetohydrodynamic shallow water equation [12,13], which has similar Hamiltonian structure as the RTSW equation.

 $\bf Acknowledgements$ This work was supported by 100/2000 Ph.D. Scholarship Program of the Turkish Higher Education Council.

References

- Afkham, B.M., Hesthaven, J.: Structure preserving model reduction of parametric Hamiltonian systems. SIAM Journal on Scientific Computing 39(6), A2616–A2644 (2017). DOI 10.1137/17M1111991
- Ahmed, S.E., San, O., Bistrian, D.A., Navon, I.M.: Sampling and resolution characteristics in reduced order models of shallow water equations: Intrusive vs nonintrusive. International Journal for Numerical Methods in Fluids 92(8), 992–1036 (2020). DOI 10.1002/fld.4815
- 3. Barrault, M., Maday, Y., Nguyen, N.C., Patera, A.T.: An empirical interpolation method: application to efficient reduced-basis discretization of partial differential equations. Comptes Rendus Mathematique 339(9), 667–672 (2004). DOI 10.1016/j.crma.2004.08.006
- Bauer, W., Cotter, C.: Energy-enstrophy conserving compatible finite element schemes for the rotating shallow water equations with slip boundary conditions. Journal of Computational Physics 373, 171 – 187 (2018). DOI 10.1016/j.jcp.2018.06.071
- Bistrian, D.A., Navon, I.M.: An improved algorithm for the shallow water equations model reduction: Dynamic Mode Decomposition vs POD. International Journal for Numerical Methods in Fluids 78(9), 552–580 (2015). DOI 10.1002/fld.4029
- Bistrian, D.A., Navon, I.M.: Randomized dynamic mode decomposition for nonintrusive reduced order modelling. Internat. J. Numer. Methods Engrg. 112(1), 3–25 (2017). DOI 10.1002/nme.5499
- Carlberg, K., Tuminaro, R., Boggs, P.: Preserving Lagrangian structure in nonlinear model reduction with application to structural dynamics. SIAM J. Sci. Comput. 37(2), B153– B184 (2015). DOI 10.1137/140959602
- Chaturantabut, S., Beattie, C., Gugercin, S.: Structure-preserving model reduction for nonlinear port-Hamiltonian systems. SIAM Journal on Scientific Computing 38(5), B837– B865 (2016). DOI 10.1137/15M1055085
- 9. Chaturantabut, S., Sorensen, D.C.: Nonlinear model reduction via discrete empirical interpolation. SIAM J. Sci. Comput. **32**(5), 2737–2764 (2010). DOI 10.1137/090766498
- Chaturantabut, S., Sorensen, D.C.: A state space error estimate for POD-DEIM nonlinear model reduction. SIAM Journal on Numerical Analysis 50(1), 46–63 (2012). DOI 10. 1137/110822724
- 11. Cohen, D., Hairer, E.: Linear energy-preserving integrators for Poisson systems. BIT Numerical Mathematics **51**(1), 91–101 (2011). DOI 10.1007/s10543-011-0310-z
- Dellar, P.J.: Hamiltonian and symmetric hyperbolic structures of shallow water magnetohydrodynamics. Physics of Plasmas 9(4), 1130–1136 (2002). DOI 10.1063/1.1463415
- Dellar, P.J.: Common Hamiltonian structure of the shallow water equations with horizontal temperature gradients and magnetic fields. Physics of Fluids 15(2), 292–297 (2003). DOI 10.1063/1.1530576
- Dempsey, D.P., Rotunno, R.: Topographic Generation of Mesoscale Vortices in Mixed-Layer Models. Journal of the Atmospheric Sciences 45(20), 2961–2978 (1988). DOI 10.1175/1520-0469(1988)045/2961:TGOMVI) 2.0.CO:2
- 15. Eldred, C., Dubos, T., Kritsikis, E.: A quasi-Hamiltonian discretization of the thermal shallow water equations. Journal of Computational Physics $\bf 379$, 1 31 (2019). DOI 10.1016/j.jcp.2018.10.038
- Esfahanian, V., Ashrafi, K.: Equation-free/Galerkin-free reduced-order modeling of the shallow water equations based on Proper Orthogonal Decomposition. Journal of Fluids Engineering 131(7), 071401–071401–13 (2009). DOI 10.1115/1.3153368
- 17. Gong, Y., Wang, Q., Wang, Z.: Structure-preserving Galerkin POD reduced-order modeling of Hamiltonian systems. Computer Methods in Applied Mechanics and Engineering $\bf 315$, 780-798 (2017). DOI $\bf 10.1016/j.cma.2016.11.016$
- Gouzien, E., Lahaye, N., Zeitlin, V., Dubos, T.: Thermal instability in rotating shallow water with horizontal temperature/density gradients. Physics of Fluids 29(10), 101702 (2017). DOI 10.1063/1.4996981
- Karasözen, B., Uzunca, M.: Energy preserving model order reduction of the nonlinear schrödinger equation. Advances in Computational Mathematics 44(6), 1769–1796 (2018). DOI 10.1007/s10444-018-9593-9
- 20. Karasözen, B., Yıldız, S., Uzunca, M.: Structure preserving model order reduction of shallow water equations. Mathematical Methods in the Applied Sciences $\mathbf{n/a}(\mathrm{n/a})$ (2020). DOI 10.1002/mma.6751

 Kurganov, A., Liu, Y., Zeitlin, V.: Thermal versus isothermal rotating shallow water equations: comparison of dynamical processes by simulations with a novel well-balanced central-upwind scheme. Geophysical & Astrophysical Fluid Dynamics 0(0), 1–30 (2020). DOI 10.1080/03091929.2020.1774876

- Kurganov, A., Liu, Y., Zeitlin, V.: A well-balanced central-upwind scheme for the thermal rotating shallow water equations. J. Comput. Phys. 411, 109414, 24 (2020). DOI 10.1016/ j.jcp.2020.109414
- Lozovskiy, A., Farthing, M., Kees, C.: Evaluation of Galerkin and Petrov-Galerkin model reduction for finite element approximations of the shallow water equations. Computer Methods in Applied Mechanics and Engineering 318, 537 – 571 (2017). DOI 10.1016/j. cma.2017.01.027
- 24. Lozovskiy, A., Farthing, M., Kees, C., Gildin, E.: POD-based model reduction for stabilized finite element approximations of shallow water flows. Journal of Computational and Applied Mathematics 302, 50 70 (2016). DOI 10.1016/j.cam.2016.01.029
- Miyatake, Y.: Structure-preserving model reduction for dynamical systems with a first integral. Japan Journal of Industrial and Applied Mathematics 36(3), 1021–1037 (2019). DOI 10.1007/s13160-019-00378-y
- Peng, L., Mohseni, K.: Symplectic model reduction of Hamiltonian systems. SIAM Journal on Scientific Computing 38(1), A1–A27 (2016). DOI 10.1137/140978922
- Qian, E., Kramer, B., Peherstorfer, B., Willcox, K.: Lift & learn: Physics-informed machine learning for large-scale nonlinear dynamical systems. Physica D: Nonlinear Phenomena 406, 132401 (2020)
- Reis, T., Stykel, T.: Stability analysis and model order reduction of coupled systems. Math. Comput. Model. Dyn. Syst. 13(5), 413–436 (2007). DOI 10.1080/13873950701189071
- 29. Ripa, P.: On improving a one-layer ocean model with thermodynamics. Journal of Fluid Mechanics 303, 169-201 (1995). DOI 10.1017/S0022112095004228
- 30. Salmon, R.: Poisson-bracket approach to the construction of energy- and potential-enstrophy-conserving algorithms for the shallow-water equations. Journal of the Atmospheric Sciences **61**(16), 2016–2036 (2004). DOI 10.1175/1520-0469(2004)061\(\cappa 2016: PATTCO\(\cappa 2.0.CO; 2\)
- 31. Ştefănescu, R., Sandu, A., Navon, I.M.: Comparison of POD reduced order strategies for the nonlinear 2D shallow water equations. International Journal for Numerical Methods in Fluids **76**(8), 497–521 (2014)
- 32. Warneford, E.S., Dellar, P.J.: The quasi-geostrophic theory of the thermal shallow water equations. Journal of Fluid Mechanics **723**, 374–403 (2013). DOI 10.1017/jfm.2013.101
- 33. Warneford, E.S., Dellar, P.J.: Thermal shallow water models of geostrophic turbulence in Jovian atmospheres. Physics of Fluids **26**(1), 016603 (2014). DOI 10.1063/1.4861123
- Wimmer, G.A., Cotter, C.J., Bauer, W.: Energy conserving upwinded compatible finite element schemes for the rotating shallow water equations. Journal of Computational Physics 401, 109016 (2020). DOI 10.1016/j.jcp.2019.109016
- 35. Young, W.R., Chen, L.: Baroclinic Instability and Thermohaline Gradient Alignment in the Mixed Layer. Journal of Physical Oceanography **25**(12), 3172–3185 (1995). DOI 10.1175/1520-0485(1995)025(3172:BIATGA) 2.0.CO;2
- 36. Zeitlin, V.: Geophysical fluid dynamics: understanding (almost) everything with rotating shallow water models. Oxford University Press, Oxford (2018). DOI 10.1093/oso/9780198804338.001.0001
- 37. Zerroukat, M., Allen, T.: A moist Boussinesq shallow water equations set for testing atmospheric models. Journal of Computational Physics **290**, 55 72 (2015). DOI https://doi.org/10.1016/j.jcp.2015.02.011
- 38. Zlatko, D., Gugercin, S.: A new selection operator for the discrete empirical interpolation method-improved a priori error bound and extensions. SIAM Journal on Scientific Computing 38(2), A631–A648 (2016). DOI 10.1137/15M1019271